Ultra-Thin, Light-Trapping Silicon Solar Cells

Geoffrey A. Landis*
NASA Lewis Research Center, 302-1
Cleveland, OH 44135

Summary

Design concepts for ultra-thin (2-10 μ) high efficiency single-crystal silicon cells are discussed. Light trapping allows more light to be absorbed at a given thickness, or allows thinner cells of a given Jsc. Extremely thin cells require low surface recombination velocity at both surfaces, including the ohmic contacts. Reduction of surface recombination by growth of heterojunctions of ZnS and GaP on Si has been demonstrated. The effects of these improvements on AM0 efficiency is shown. The peak efficiency increases, and the optimum thickness decreases. Cells under 10 μ thickness can retain almost optimum power.

The increase of absorptance due to light trapping is considered. This is not a problem if the light-trapping cells are sufficiently thin.

Ultra-thin cells have high radiation tolerance. A 2 μ thick light-trapping cell remains over 18% efficient after the equivalent of 20 years in geosynchronous orbit. Including a 50 μ thick coverglass, the thin cells had specific power after irradiation over ten times higher than the baseline design.

Introduction

Recent advances in silicon solar cell technology has resulted in cell efficiencies [ref. 1,2] as good or better than those obtained by competing technologies. Advances in efficiency, power/weight, and radiation tolerance for next-generation silicon space cells space use will require reducing the thickness. As thickness is decreased, the effect of surface recombination at both front and back surfaces becomes increasingly important; ultra-thin silicon cells will require both surfaces to be passivated, including the ohmic contacts. To avoid loss of short circuit current, an optical confinement structure will be required [ref. 2].

We have thinned silicon wafers to under 10μ without breakage. Thinner cells may require special handling, or will have to be bonded to a substrate (or superstrate) for processing.

Light Trapping

Light trapping techniques increase the pathlength of light within the cell, allowing more of the light to be absorbed at a given thickness, or allowing thinner cells of a given J_{sc}. Several light trapping geometries have been proposed [ref. 3,4,5]. One effective light trapping geometry is the cross-grooved structure proposed by the author [ref. 6] and recently analyzed by Campbell and Green [ref. 7]. This is shown in figure 1. The grooved geometry has the low reflectivity typical of textured cells.

Figure 2 shows a ray-tracing of the path travelled by a typical light ray. A figure of merit for optical confinement is the average path length for weakly absorbed light. For random (Lambertian) confinement, this pathlength is $4n^2$ times the thickness [ref. 4], where n is the refractive index. $4n^2$ equals about 50 for silicon in the wavelenghts of interest. For the cross-grooved geometry, the effective light trapping is slightly better, since all of the light is confined for the first two round-trip passages, a pathlength of about 8 times the thickness. After this the light is nearly randomized in direction. The average pathlength is thus about $4n^2 + 8$ times the cell thickness. This is similar to the results of Campbell and Green's ray-tracing analysis [ref. 7], who show an optical path length of 52-72 times the thickness, depending on groove spacing to width ratio.

This difference is more important at shorter wavelengths, since the first four round-trip passages are more important.

Modelling Light Trapping

The increases in optical pathlength are due to three effects: back surface reflection (BSR), oblique passage of light through the cell, and geometry-related trapping reducing the probability of a ray exiting.

The BSR is modelled simply as an additional light source illuminating the cell from the back with intensity $I = I_o\ exp(-\alpha_{eff}\ T)$. This effectively doubles the pathlength for weakly absorbed light.

Oblique light passage is modelled as an increase in the absorption constant; $\alpha_{eff} = \alpha/cos\theta$. For fully randomized light, θ_{ave} is 60°, and the effective absorption constant is doubled.

Confinement geometry is modelled as an effective increase in light intensity inside the cell. If the escape probability of a ray incident on the interior surface is B, then the average pathlength increase factor is 1/B, and the (wavelength-dependent) effective intensity increase is:

$$I' = \frac{1}{1-(1-B^{-1})e^{-2\alpha_{eff}T}} \tag{1}$$

For Lambertian confinement, $B=n^{-2}$. Figure 3 shows this geometrical enhancement factor versus αT, cell thickness T measured as a multiple of the absorption depth α^{-1}. The factor approaches the asymptotic limit $n^2 \approx 12.5$ at very low thicknesses (or long absorption depths). Oblique light passage and back surface reflection (BSR) together contribute a further enhancement, a factor of 4 in the weakly-absorbed limit. (For the cross-grooved geometry, the effect of the first two fully-trapped passes must also be included.) The enhancement factor is low for higher absorption constants because most of the light is already absorbed in the first few passages. Clearly, the effective enhancement is only important for very short cell thicknesses, or for very low absorption (long wavelength) light.

Absorptivity

Thermal alpha is an important consideration for space solar cells, since the higher the absorption, the higher the cell operating temperature will be. Unless the cells are covered with an IR-rejection filter, this will vary greatly with the absorption of sub-bandgap IR light. A light trapping structure very effectively increases the pathlength for weakly absorbed light, thus increasing alpha.

Calculated absorptivity will depend greatly on the absorption length of IR light in the silicon, which is dependant on silicon quality, oxygen and carbon content, doping level, etc. Figure 4 shows an idealized result, calculated assuming that the sub-bandgap light had an absorption depth α^{-1} for sub-bandgap light of 5000 μ. The figure compares a structure with light trapping effectiveness of 50 times the thickness with an ideal gridded-back contact cell, modelled here as a once-through design. (An actual gridded-back cell will have slightly higher absorption, since the back will not actually be fully transparent.) Cell temperatures shown on the right side are calculated using data from Garlich and Lillington [ref. 8]. The result of the light-trapping is to shift the absorption to lower thicknesses. The 5 μ light-trapping cell shown has the same absorption as the 250 μ gridded-back cell.

Grid Shadowing

An additional gain can be realized when the contact metallization is highly reflective, and applied to only one of the groove sides, as shown in figure 1 (proposed by Borden and Walsh, [ref. 9]). Incident light striking the metallized portion reflects onto the opposite side and enters the cell. A variant geometry is to run the contact lines at an angle across the groove [ref. 10]. All of these techniques can result in elimination of the effective grid shadowing.

Surface Passivation

Extremely thin cells also require the surface recombination velocity S to be low at both front and back surfaces. As noted by Lindholm *et al.* [ref. 11], a small area of surface with high recombination velocity will degrade the efficiency of the cell much more than proportionately to the area. While oxide passivation has been shown to result in surfaces of extremely low S [ref. 12], SiO_2 is non-conductive and thus the technique must leave the surface unpassivated at the ohmic contacts. We have proposed [ref. 13] reduction of the surface recombination velocity of Si by use of a heterojunction window layer such as is used on GaAlAs/GaAs cells. The theoretical band diagram of an ideal heterojunction-passivated cell is shown in figure 5. ZnS (lattice constant 5.41Å, bandgap 3.6 eV) and GaP (lattice constant 5.41Å, bandgap 2.3 eV) are the available wide-bandgap semiconductors which are lattice matched to silicon. Of the two, ZnS is a preferable choice for the front window layer, since the bandgap of 3.6 eV results in nearly complete transparancy to the solar spectrum. The slightly narrower bandgap of GaP could result in as much as 10% reduction in I_{sc} unless the layer is extremely thin.

ZnS is an excellent AR coating material, with a measured refractive index of 2.2 to 2.3 for the films we deposited. It can only be doped n-type. We have grown ZnS heterojunctions onto solar cells by vacuum evaporation [ref. 4]. Figure 6 shows a typical cell quantum efficiency. An elevated substrate temperature is required for growth; this result was done with the substrate temperature of 450° C. The growth rate was about 100Å/min. This was done on a textured surface; similar results were also obtained on planar (100) surfaces. Three quantum efficiency curves are shown, that of the cell with an oxide passivation, that of the same cell with the oxide stripped, and that of the same cell again, after ZnS was deposited. The lowered surface recombination can be seen in the increased response at short wavelengths and in an increased open circuit voltage compared to the bare cell. S does not appear to be quite as low as the value obtained by thermal oxidation, although it is considerably better than that obtained on the bare surface. No decrease is seen in long wavelength response, indicating no degradation in bulk minority carrier lifetime.

Similar reductions of surface recombination velocity have been shown for films of ZnS and GaP on Si grown at Spire Corporation by MO-CVD [ref. 15,16]. Figure 7 shows the spectral response of a GaP coated cell compared to a control cell. Growth tempertature here was 675° C. The absorption cut-on of the GaP is quite clear. When the curves are corrected for absorption in the GaP, the increase in short-wavelength quantum efficiency is quite clear. Again, no decrease is seen in the bulk lifetime

We expect that lower surface recombination velocity can be achieved with improvements in ZnS deposition methods. If this is not achieved, however, an alternate structure is proposed where a thermal oxide is grown on the surface and holes etched at small-area spots for ZnS growth where the contacts are to be made.

Cell Performance Modelling

Solar cell performance was modelled using a computer program that calculated a four-layer solution to the transport equations, based on the analyses of Wolf [ref. 17], Godlewski [ref. 18], and others. Sample calculations were also run with a finite element simulation [ref. 19] to check the model validity. Figure 8 shows results of computer modelling of advanced cell performance at AM0. The cell modelled was a n on p configuration, with $x_j = 1\mu$, emitter doping $10^{19}/cm^3$, and base doping $10^{17}/cm^3$. Representative doping levels were chosen to avoid extremes of heavy-doping and bandgap narrowing; the junction depth and doping was not optimized for the thin cell. In all of the cases shown the front and back surfaces were assumed to be passivated with S=10 cm/sec. The model neglects external losses such as grid coverage, reflection, etc., which in any case will presumably be small, due the use of textured front surface and zero grid-shadow geometry. The effect of light trapping is to increase the peak efficiency of the cell and to decrease the optimum cell thickness.

Radiation damage was modelled by assuming diffusion length degradation according to the formula [ref. 20]:

$$L^{-2} = L_o^{-2} + K_L \Phi \tag{2}$$

where Φ is the radiation fluence. For 1 MeV electrons, the value for K_L assumed was $5 \cdot 10^{-9}$, a value typical of the highly doped substrates modelled. Figure 9 shows the cell power after a

radiation dose of 10^{15} electrons/cm^2. After radiation damage the thin cells have considerably higher power than the thick ones. The 2μ cell retains 77% of its initial power after 10^{15} electrons/cm^2, corresponding to roughly 20 years in geosynchronous orbit. Greater radiation fluences result in even greater advantage to the thin cells.

An important figure of merit for space solar cells is the power to weight ratio, or specific power. Figure 10 shows the comparative specific power of these cells after irradiation, assuming a 50 μ thick coverglass. Using thin cells and covers, it should be possible to achieve EOL cell specific power targets of well over 1000W/Kg.

Conclusions

Ultra-thin cells with light trapping and surface passivation can increase the efficiency and radiation tolerance of silicon cells markedly. A 2 μ thick light-trapping cell remains over 18% efficient after the equivalent of 20 years in geosynchronous orbit. Including a 50 μ thick coverglass, the thin cells had specific power after irradiation over ten times higher than the baseline design.

Acknowledgements

I would like to thank some of the people who contributed to the results presented here, in particular Stan Vernon, Patricia Sekula, Chris Keavney and Mark Spitzer at Spire, and Roland Beaulieu and Joseph Loferski at Brown.

**Portions of this work were done while the author held a National Research Council Research Associateship at NASA Lewis Research Center. Other portions were done at Brown University in collaboration with Spire Corporation, supported in part by DOE.*

References

[1] R.A. Sinton et al., *18th IEEE Photovoltaic Specialists Conference*, p. 61-65 (1985)

[2] M.A. Green, S.R. Wentham and A.W. Blakers, *19th IEEE Photovoltaic Specialists Conference*, 6-12 (1987).

[3] M.B. Spitzer, Ph.D. Thesis, Brown University; M.B. Spitzer *et al.*, *14th IEEE Photovoltaic Specialists Conference* , 375-380 (1980).

[4] E. Yablonovitch and G.D. Cody, IEEE Trans. Electron Dev., ED-29:2, 300 (1982).

[5] D. Redfield, Appl. Phys. Lett., **35** 11, 647-648 (1974).

[6] G.A. Landis, Cross-grooved Solar Cell, U.S. Patent No. 6,608,451 (1986).

[7] P. Campbell and M.A. Green, J. Appl. Phys, **62** 1, 243-249 (1987).

[8] G.F. Garlich and D.R. Lillington, *Space Photovoltaic Research and Technology 1986*, NASA CP 2475, 87-97, (1986).

[9] P.G. Borden and R.V. Walsh, Appl. Phys. Lett., **41** 1, 649-651 (1982).

[10] M.A. Green et al., *19th IEEE Photovoltaic Specialists Conference*, 49-52 (1987).

[11] F.A. Lindholm et al., Solid State Electronics **23,** 967-971 (1980).

[12] M.B. Spitzer *et al.*, 17th IEEE Photovoltaic Specialists Conference, 398-402 (1984); L.C. Olsen et al., *17th IEEE Photovoltaic Specialists Conference*, 403-408 (1984); A. Rohatgi et al., *17th IEEE Photovoltaic Specialists Conference*, 409-414 (1984).

[13] G.A. Landis, PhD. Thesis, Physics Department, Brown University (1988);

[14] C. Case et al., *19th IEEE Photovoltaic Specialists Conference*, 398 (1987).

[15] P. Sekula et al., "Reducing the Surface Recombination Velocity of Silicon Solar Cells", *Spire Corporation, Final Report for U.S. Department of Energy*, July 1987.

[16] M.B. Spitzer, S. M. Vernon, and C.J. Keavney, "Development of Gallium Phosphide Heteroface Back Surface Field Structures", *Spire Corporation, Final Report for NASA Lewis Research Center Contract NAS3-24642*, October 1986.

[17] M. Wolf, *14th IEEE Photovoltaic Specialists Conference*, 563-568 (1980).

[18] M.P. Godlewski, C.R. Baraona, and H.W. Brandhorst, Jr., *10th IEEE Photovoltaic Speicalists Conference*, 40-49 (1973).

[19] PC-1D Computer Program, Available from Iowa Microelectronics Center. See D.T. Rover, P.A. Basore and G.M. Thorson, *18th IEEE Photovoltaic Specialists Conference*, p. 703 (1985).

[20] *Solar Cell Radiation Handbook, Third edition*, JPL Publication 82-69 (1982).

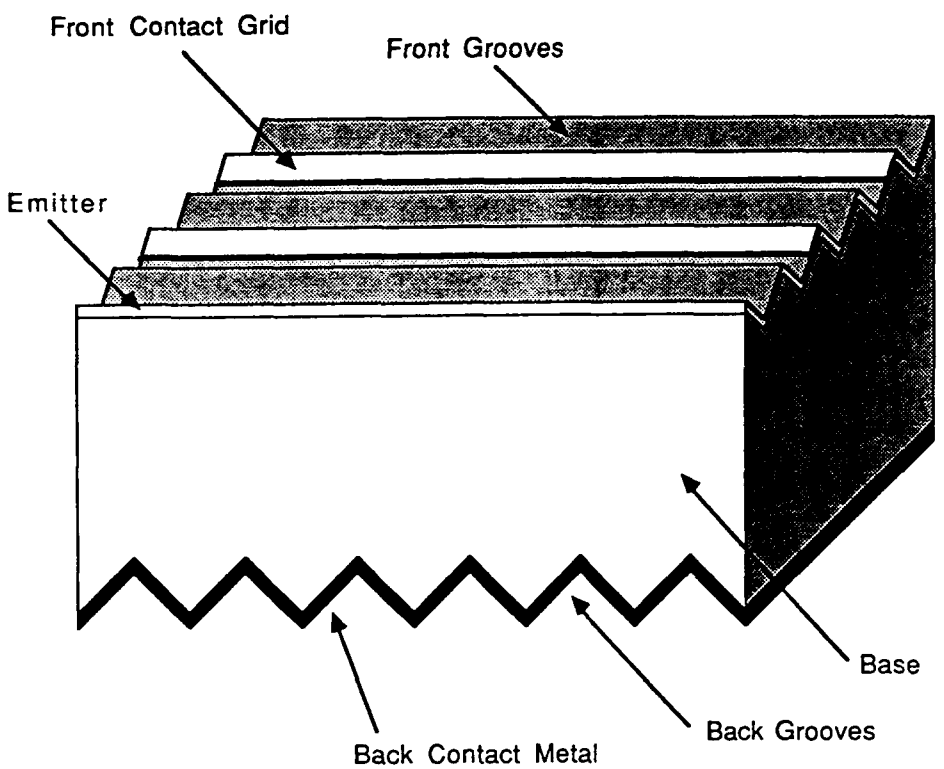

Figure 1. Schematic of solar cell incorporating cross-grooved light-trapping geometry.

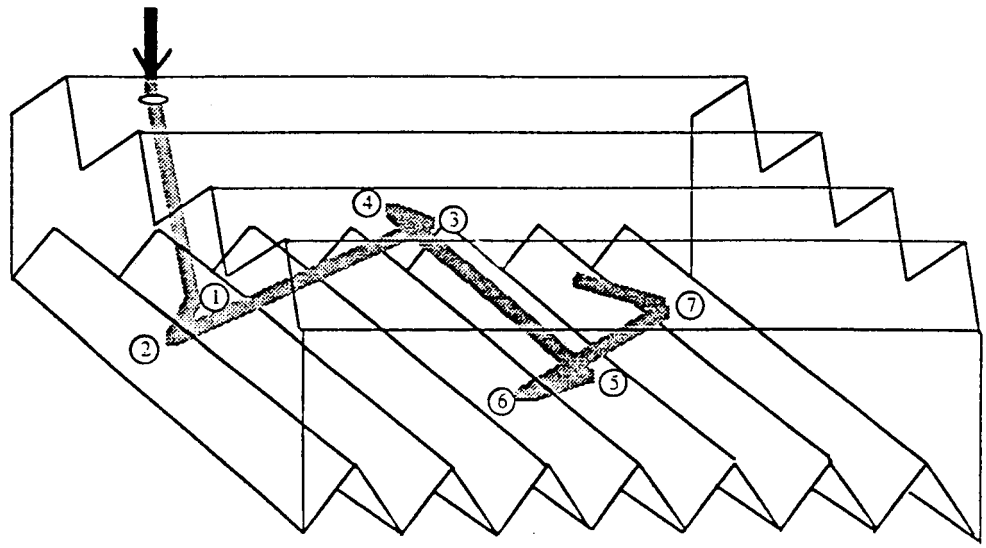

Figure 2. Typical ray passage in cross-grooved geometry, showing typical light path for first two passages through cell.

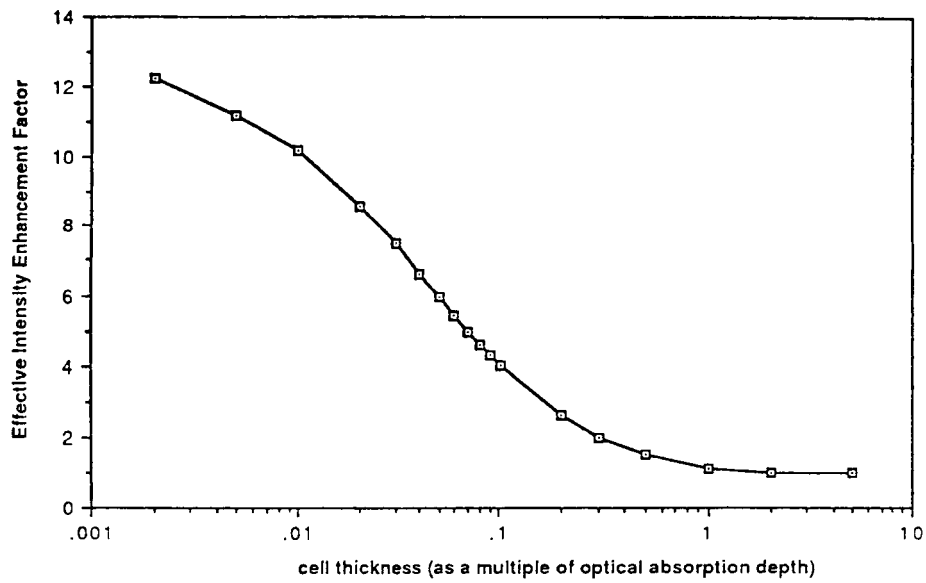

Figure 3. Effective intensity enhancement due to geometrical light trapping (not including effects of oblique passage or BSR) as a function of αT.

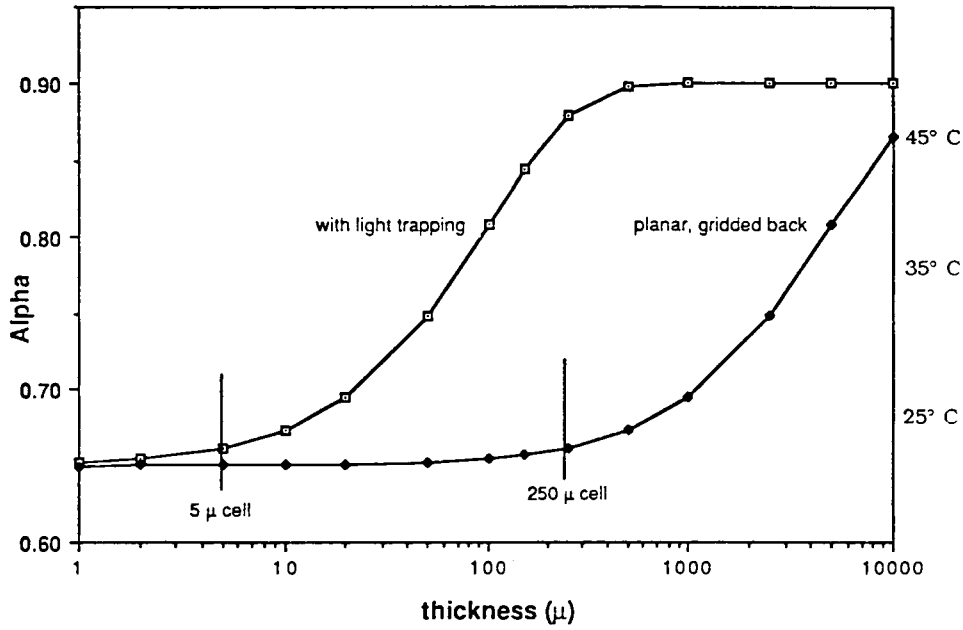

Figure 4. Idealized thermal α versus cell thickness for light trapping cell and gridded back contact cell.

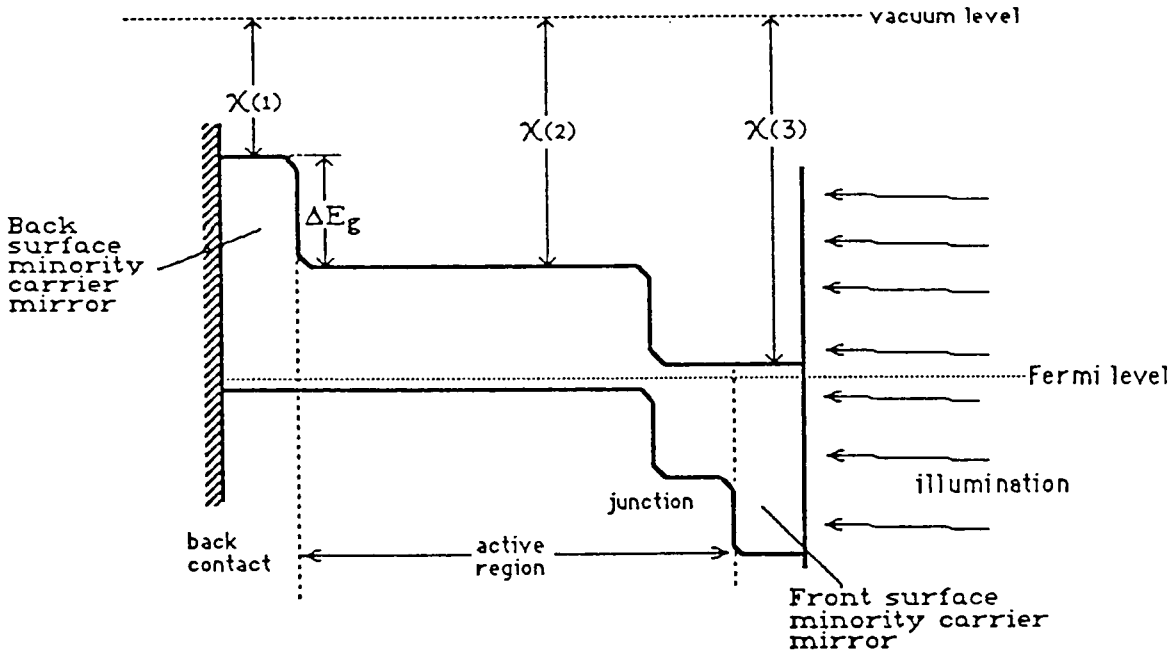

Figure 5. Idealized band diagram for heterojunction passivated solar cell.

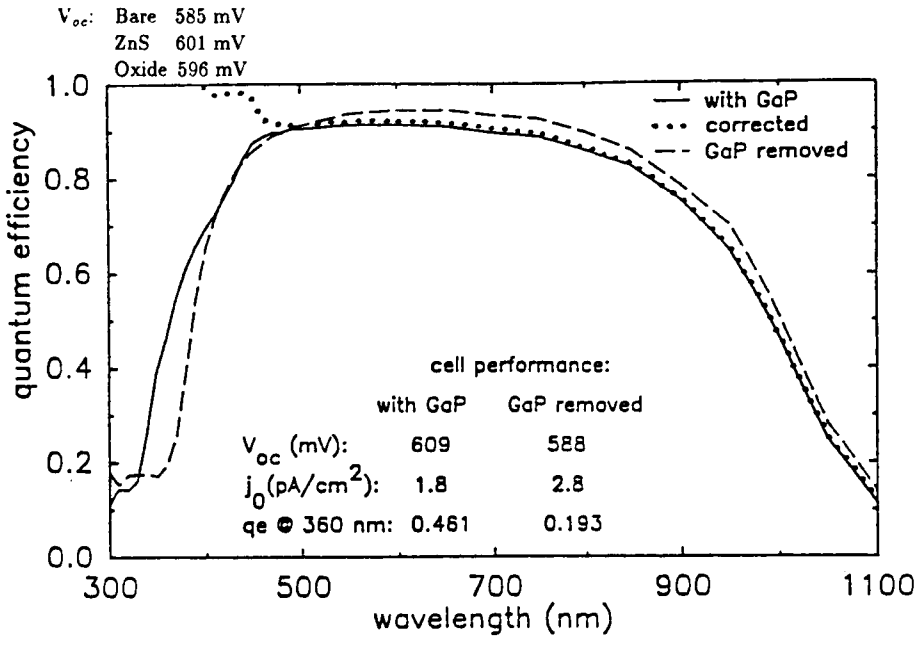

Figure 6 (External) Quantum Efficiency of Si cell with zinc sulfide heterojunction window grown by vacuum deposition, showing response of bare cell, cell with thermal SiO_2, and cell with ZnS window (measurement courtesy Spire Co.)

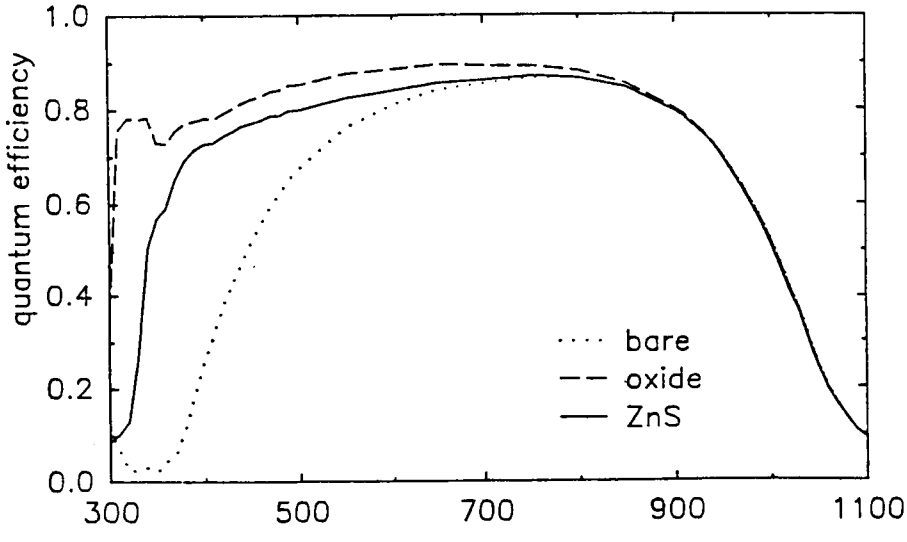

Figure 7. (External) Quantum Efficiency of Si cell with MO-CVD deposited gallium phosphide heterojunction window, showing response of bare cell, cell with GaP, and cell with GaP after correction for absorption in window layer (figure courtesy Spire Co.).

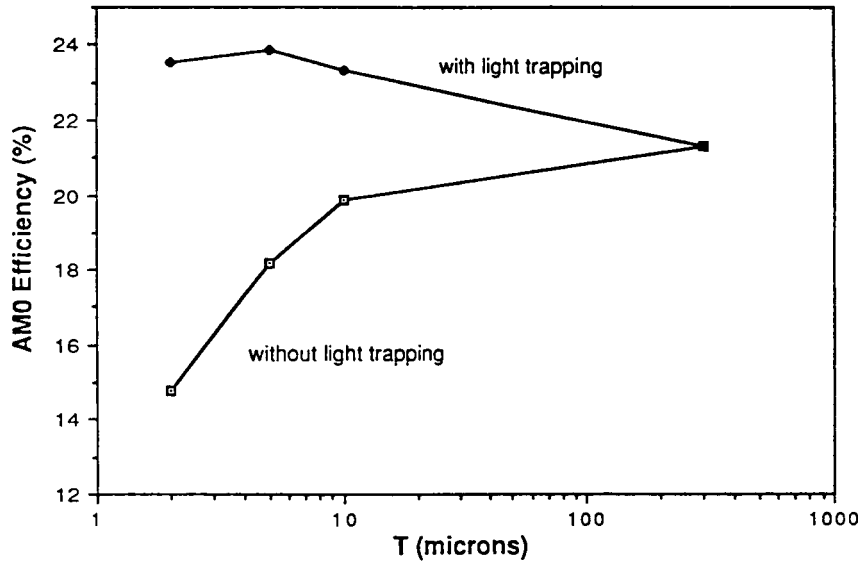

Figure 8. Calculated AMO Efficiency versus thickness for Si cells with and without light trapping.

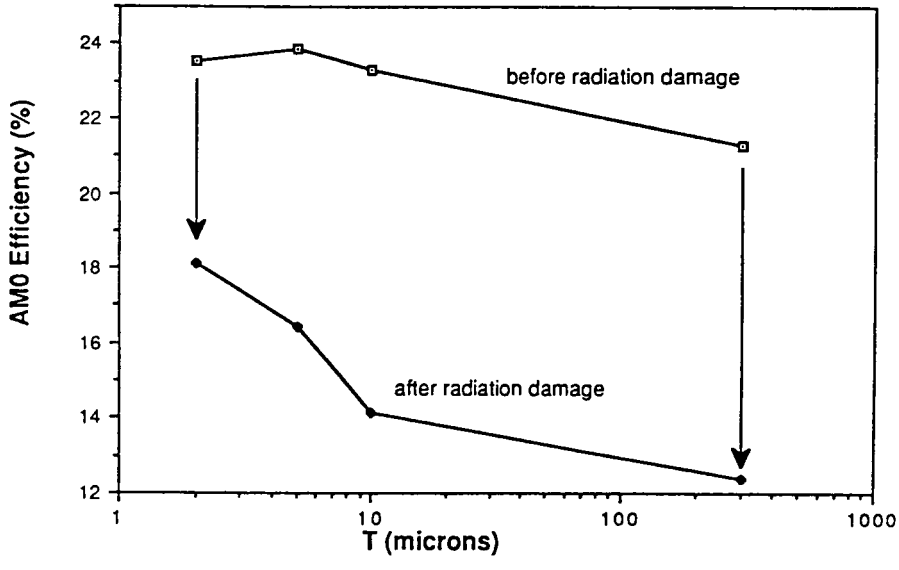

Figure 9. Calculated AMO Efficiency versus thickness for Si cells with light trapping, before and and after 10^{15} 1-MeV electron/cm^2 irradiation.

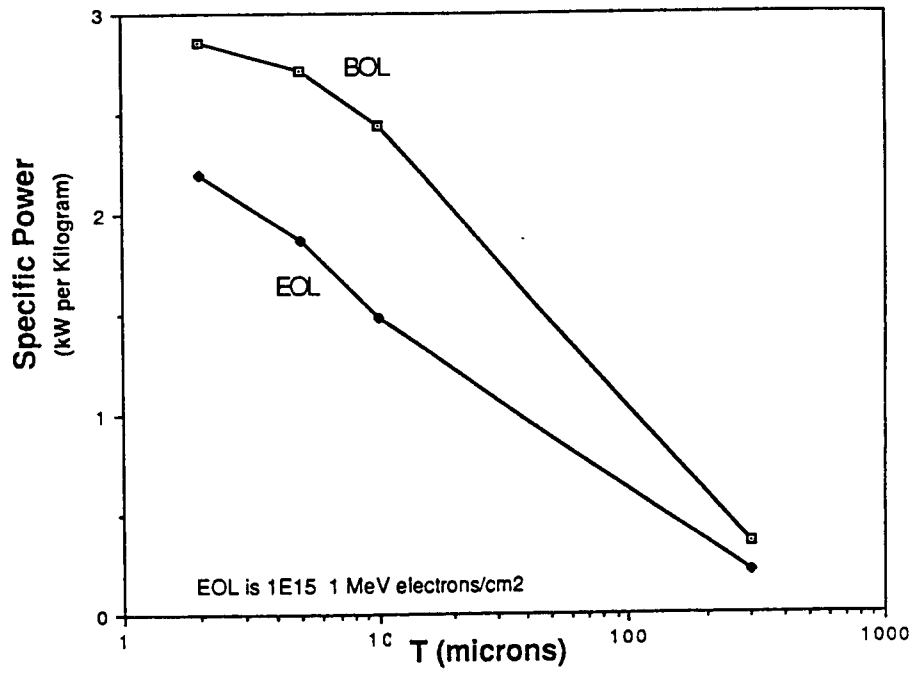

Figure 10. Cell specific power as a function of thickness, at beginning of life and after 10^{15} 1-MeV e^{-}/cm^{2} (includes 50 μ glass cover).